JOURNAL OF MATERIALS SCIENCE 15 (1980) 2354–2364

The measurement of shear compliances for oriented polyethylene terephthalate sheet

E. L. V. LEWIS, I. M. WARD
Department of Physics, University of Leeds, Leeds, UK

Two techniques have been used to measure the shear compliances of one-way drawn uniplanar-axially-oriented polyethylene terephthalate (PET) sheet, draw ratio 5:1; a torsional method for all three compliances S_{44}, S_{55} and S_{66}, and a recently-developed simple-shear method for S_{44} and S_{66}. The two techniques gave values for the compliances in common which agreed very well. An examination of end effects in torsion has also been made. The determination of the three shear compliances complete the determination of all nine independent compliances for this PET sheet. The overall mechanical anisotropy has been considered in the light of existing structural information, and comparison made with the elastic constants of isotropic PET and a highly oriented PET fibre on the basis of the single-phase aggregate model.

1. Introduction

In previous papers the determination of six of the nine independent elastic constants of one-way drawn polyethylene terephthalate (PET) sheet (sheet I) have been described [1–3]. The determination of the three shear compliances was also described in an earlier publication for a similar but not identical PET sheet (sheet II) [4]. The method adopted for the measurement of the shear compliances was torsion of thin strips cut from the sheet. Recently we have developed a new technique for the determination of shear compliances [5]: a simple-shear method where the shear displacement is measured by the movement of magnets with a Hall plate. In the present paper we describe the determination of the three shear compliances for the PET sheet I. Both the simple-shear method and the torsion of thin strips have been used. In addition, the effect of the ends in torsion has been examined. In this way it has been possible to obtain final accurate values for the shear compliances with considerable confidence, and at the same time to examine critically both techniques and devise accurate procedures.

There are two important aspects of this work. Firstly, it is the first application of the new simple-shear method to anisotropic polymer sheets. The very high anisotropy of this PET sheet and the comparatively low time dependence (creep) [4] make it a very suitable material for testing the simple-shear method and making the comparison between different measurement techniques. Secondly, the measurements of the shear compliances of the PET sheet I complete the determination of all nine independent elastic constants for this material. This will enable us to make a comprehensive view of its mechanical anisotropy in terms of its structure.

2. Experimental procedure

2.1. Samples

The material in this investigation was the one-way drawn PET sheet I used for previous measurements of extensional and lateral compliances [1–3]. It was prepared by drawing isotropic sheet at constant width to a draw ratio of 5:1 at about 80° C. Wide-angle X-ray diffraction patterns are shown in Fig. 1. Following much previous work on similar materials in our laboratories [1–4, 6–9] and elsewhere [10–12], it has been shown that there is both a high degree of chain orientation in the draw direction and that the (1 0 0) crystal planes are preferentially oriented into the plane of the sheet. This type of orientation has been described as uniplanar-axial [10], and we will see that the mechanical anisotropy is a remarkable reflection of this. In some of our previous papers we have described the sheet as possessing orthorhombic

 0022–2461/80/092354–11$03.10/0

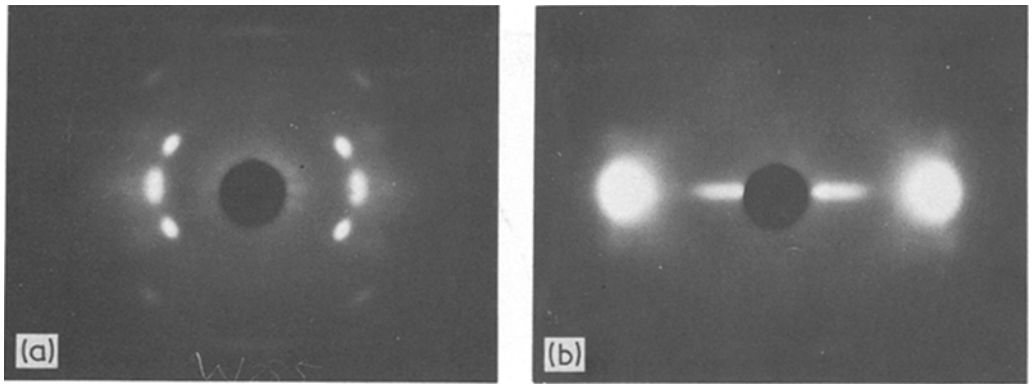

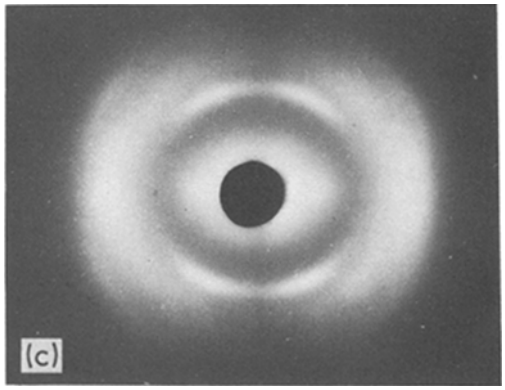

Figure 1 Wide-angle X-ray diffraction patterns for the PET sheet: (a) normal to the sheet, fibre axis vertical; (b) parallel to the sheet, fibre axis vertical; (c) along the fibre axis, sheet plane vertical.

symmetry. This is strictly true in the sense that the sheet possesses three orthogonal planes of symmetry, but it is less descriptive than uniplanar-axial.

For the torsion measurements all samples were cut from the central region of the sheet where thickness (~ 0.25 mm) and properties were constant. We have followed the following conventions [1–5] in defining axes and elastic constants. The draw direction is termed 3 or z, the normal to the plane of the sheet 2 or y, and the transverse direction 1 or x; for samples cut from this sheet the length, width and thickness will be denoted by l, w and t respectively (Fig. 2). The elastic behaviour of anisotropic samples at small strains is given by the generalized Hooke's Law in matrix notation

$$\epsilon_i = \sum_{j=1}^{6} S_{ij}\sigma_j, \qquad (1)$$

where ϵ_i are the strains, σ_j the stresses, and S_{ij} the corresponding compliances (reciprocals of the moduli). Values of $j = 4$, 5 or 6 refer to shear of the planes normal to 1, 2 or 3 respectively. For uniplanar-axial samples there are nine independent non-zero compliances: S_{11}, S_{22} and S_{33} referring

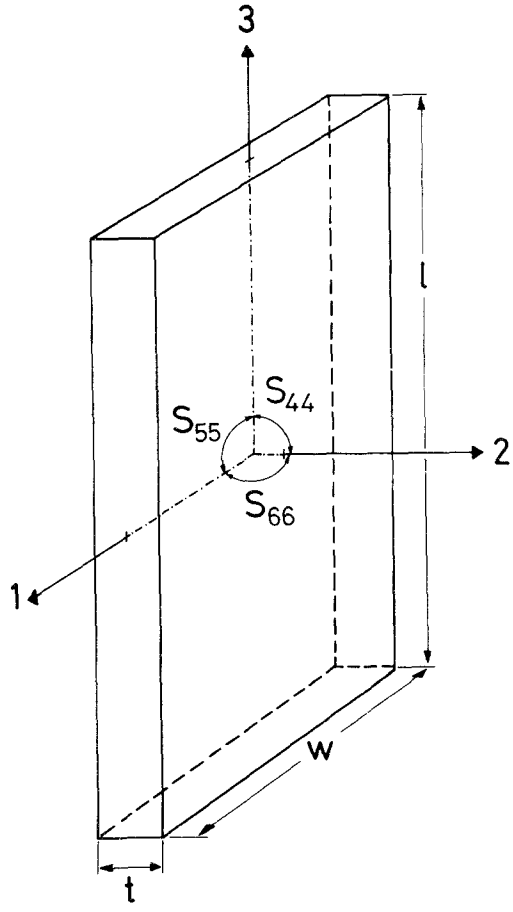

Figure 2 Diagrams showing Cartesian axes with respect to sample sheet: 3 is parallel to the initial draw direction, 2 is normal to the sheet, and 1 is the transverse direction. The shear compliances S_{44}, S_{55} and S_{66} correspond to shear in the planes normal to the 1, 2 and 3 directions respectively. For a sample cut perpendicular to the initial draw direction, l and w will be interchanged.

to extension or compression; S_{12}, S_{13} and S_{23} which are related to the Poisson's ratios ν_{ij} by the relation $\nu_{ij} = -S_{ij}/S_{jj}$; and the shear compliances S_{44}, S_{55} and S_{66}. We shall be dealing with this last set in this paper.

2.2. Apparatus

2.2.1. The torsion method

The torsion apparatus is based on the design of Raumann [13] and has been described in earlier papers [4, 14–16]. The Saint–Venant theory of torsion was used to calculate two estimates of the shear compliance in the plane of the sheet, $\overline{S^z_{55}}$ and $\overline{S^x_{55}}$ (the bar denoting Saint–Venant treatment); these were obtained from twisting rectangular samples cut out with their long axes parallel to z and x respectively. They were combined to form the final value $\overline{S_{55}}$. It is also possible to obtain the compliances S_{44} and S_{66} from the z-axis and x-axis samples respectively and appropriate treatment of the Saint–Venant theory [4, 16]; these will be called $\overline{S^z_{44}}$ and $\overline{S^x_{66}}$. The sample was held in grips similar to those of the extension apparatus described elsewhere [17], except that they could accept wider samples (up to 5.2 mm).

2.2.2. The simple-shear method

The simple-shear technique has been described fully elsewhere [5]. Two identical samples are held between rigid brass plates and a central brass block which can be displaced downwards. Loading the block applies a shear force to the samples which deform in simple shear. It carries a magnet which moves away from a like opposed magnet built into the apparatus frame. This movement causes a change in the magnetic field between them which is detected and measured by a Hall plate mounted in the frame. The displacement is measured after suitable calibration. The compliances measured by this technique for anisotropic samples will be S_{44} for z-axis samples and S_{66} for x-axis samples, so that this method complements the torsion method.

2.3. End or length effects

2.3.1. End or length effects in torsion

There are three effects which may be present when rectangular prisms are twisted about a symmetry axis. They all cause the sample to be stiffer than it would otherwise be.

(1) Extension of lines parallel to the twist axis at the sample edge with respect to similar lines nearer the centre. This involves the extensional compliance parallel to the twist axis. It is related to the bifilar or multifilar effect in suspensions.

(2) Bending of edges at the grips. This is like a cantilever effect and so involves mainly the same extensional compliance.

(3) Planes normal to the twist axes warp into characteristic patterns, but the grips at each end prevent such warping locally. Timoshenko and Goodier [18] showed that this results in an effective increase in the stiffness given by

$$\Lambda = \left[1 - \frac{5^{1/2}(1+\nu)^{1/2}}{6}\frac{w}{l}\right]^{-1}, \quad l \gg w \gg t, \quad (2)$$

where ν is the Poisson's ratio. The normal stresses caused by this restriction decay away exponentially from the ends in a way similar to those in the theoretical analysis of Horgan [19–22].

Work on the highly anisotropic Kraton 102 by Folkes and Arridge [23] showed that the overall sample compliance did decrease as the sample length was reduced. They proposed a model in which the effects of the ends were confined to a block with sample compliance S' and length p at each end of the sample, the central region of homogeneous stress having sample compliance S^0. This gave a linear variation of measured overall sample compliance S with reciprocal length [17]

$$S = S^0 + (2p/l)(S' - S^0) \quad (l \leqslant 2p) \quad (3)$$

until the length l was so short that the two end blocks met ($l = 2p$), after which S was constant and equal to S'. Their results fitted this model, and they found that S'/S^0 was 0.298 (from a simple shear-lag theory $S'/S^0 = 0.5$).

It was decided to make similar measurements in torsion on the PET sheet I and analyse the results using the block model. This was suggested by the form of earlier torsional results on other PET sheets II [4] where the measured values of S^z_{55} and S^x_{55} fell linearly with increasing w/t ratio. This is the behaviour one would predict from the block analysis: since t and l were constant ($l \sim 35$ mm), $w/t \propto w/l$.

Wilson [8] has carried out some torsional measurements on the present PET sheets I. His preliminary results showed that $\overline{S^z_{55}}$ did decrease somewhat with decreasing length, but was constant above 80 mm; then using samples 80 mm long the graphs of S^z_{55} or S^x_{55} against aspect ratio w/t showed a curved shape (compare with [14]) rather than the straight lines seen in the earlier PET sheet [4]. However, Wilson's samples were all measured

at constant total twist ϕ_{SM}, so that no account was taken of any variation in the sample compliances with twist angle per unit length θ_{SM}. We therefore investigated the twist-dependence of sample compliances, to correct Wilson's readings to zero twist (zero strain), and to extract any end effects from the results.

2.3.2. *End or length effects in simple shear*

In the simple-shear apparatus there is a shear-lag effect similar to that in fibre-matrix composites and adhesive joints [24] but this was found to cause negligible error in the results obtained for polyethylene (PE) [5]. End effects in the samples of the kind described by Read [25] had been examined by varying the length of the samples used but were found to be negligible for the thickness used (1.8 mm); both these effects should be even less important for the present PET samples where the thickness is only 0.25 mm.

3. Results

The detailed procedures for both techniques have been described elsewhere [4, 5, 14, 16], so that only relevant features will be mentioned here.

3.1. Torsion results

Since Wilson had already studied the variation of behaviour with sample width [8], only two extreme widths were used here in both z and x directions for the variation of sample compliance with twist and with length; the widths of these fresh samples were, for the z axis: 4.57 mm (z_w) and 1.92 mm (z_n); and for the x axis: 4.64 mm (x_w) and 1.63 mm (x_n). After mounting in the apparatus, each sample was conditioned mechanically to ensure reproducibility [16] before readings were taken. The variation of torsional rigidity per unit length (M' value) with axial load (axial stress σ_A) was then measured at 0.36 rad. sample twist ϕ_{SM} and found to be linear (Fig. 3). The M value (M' value at $\sigma_A = 0$) was determined by extrapolation to $\sigma_A = 0$. The variation of M' with twist angle ϕ_{SM} was next measured and was found to be considerable (Fig. 4); three axial loads were found to be sufficient. Graphs of these results enabled the variation of the M values with ϕ_{SM} to be found for each sample. Then each sample was cut to a shorter length, reconditioned, and the procedure repeated down to the shortest lengths that could be dealt with (2–3 mm).

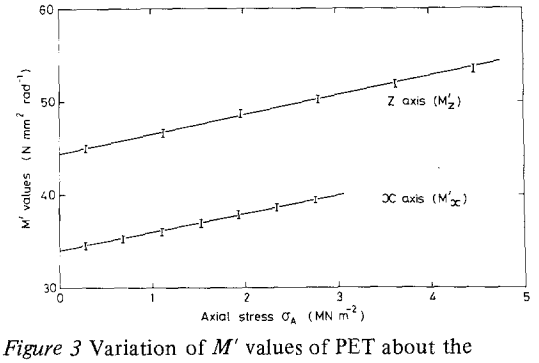

Figure 3 Variation of M' values of PET about the z- and x-axis as a function of axial stress. Sample twist of 0.36 rad.

The M values at zero twist (M^0 values) thus obtained were used to calculate the overall elastic compliance S^z_{55} (about the z-axis) or S^x_{55} (x-axis) using the Saint–Venant relations

$$S^z_{55} = \beta\left(\frac{w}{t}\sqrt{\frac{S_{55}}{S_{44}}}\right) wt^3/M^0_z; \quad (4)$$

$$S^x_{55} = \beta\left(\frac{w}{t}\sqrt{\frac{S_{55}}{S_{66}}}\right) wt^3/M^0_x, \quad (5)$$

where β is the Saint–Venant function [14, 4, 6]. The overall elastic compliance is that calculated with the argument of β equal simply to w/t; it is equivalent to assuming that $S_{44} = S_{55} = S_{66}$ as in the procedure for calculating S_{55} called the pseudo-isotropic method [14, 4, 6]. The results are given in Fig. 5 and all four samples showed an initial linear drop in overall elastic compliance with increasing reciprocal length, just as Folkes and Arridge [23] found, the effect being greater for wider samples. The block model predicts a levelling off as the length is reduced; this can be seen in the z-axis samples but no evidence of it was found in the x-axis samples even at the shortest lengths. Thus the "end blocks" seem to be longer in the former, which is as exptected from the Horgan theory [19, 20]. The lengths at which the cut-off starts are surprisingly short: for the wider sample (z_w) cut-off begins at about 6.2 mm, and for the narrower sample (z_n) it begins at about 5.5 mm. The ratio of these two, 1.1, is less than the ratio of the widths of these samples (2.38). This suggests that a more complex formula than Horgan's is probably required for flat samples, involving the thickness as well as the width.

The effect of correcting the M_z and M_x values to zero twist and infinite length was then determined. It was done first for all the fresh samples as a check on the validity of the procedure. The

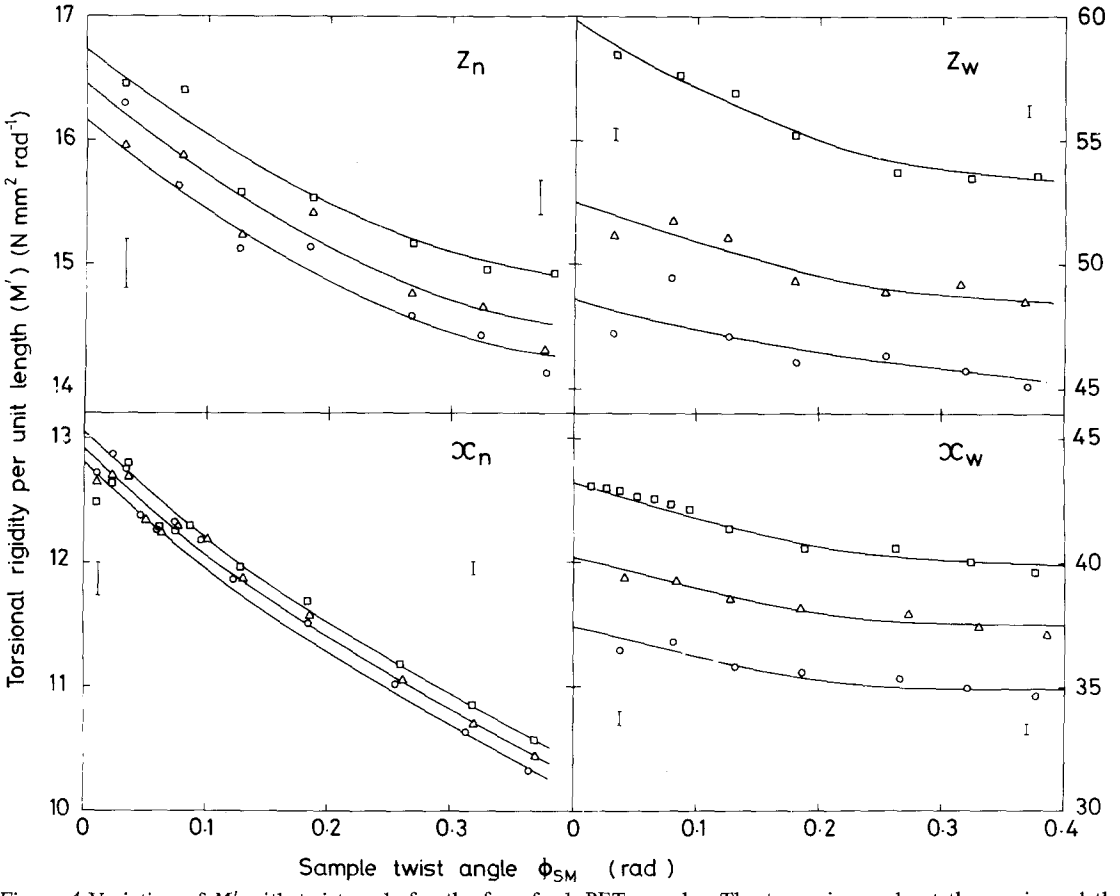

Figure 4 Variation of M' with twist angle for the four fresh PET samples. The top pair are about the z-axis, and the bottom pair about the x-axis, subscripts n and w referring to narrower and wider respectively; □, △ and ○ denote maximum, intermediate and minimum axial stress respectively. The error bars show the standard error of all three sets of points at the ϕ_{SM} value where they appear, and the curves were drawn by eye through the points and used to extrapolate to zero twist.

ratio of M for Wilson's [8] θ_{SM} value to that at zero twist was found to be independent of axial stress and length. The resulting ratios R are given in Table I. The M^0 values were calculated by putting Wilson's measured values [8] ($S_{55} = 6.1 \times 10^{-10}$ m^2 N^{-1}, $S_{44} = 95 \times 10^{-10}$ m^2 N^{-1}, $S_{66} = 132 \times 10^{-10}$ m^2 N^{-1}) into Equations 4 and 5, and then multiplying by the appropriate R (Table I). The graphs of Fig. 5 were next used to correct the M^0 to infinite length to remove end effects (Table I). The elastic compliances corresponding to these were then calculated from Equations 4 or 5 by an iterative procedure. It was found that putting starting values of S_{55} and S_{44} into Equation 4, calculating a new S_{55}, putting that back into Equation 4 and then recalculating always produced values which converged to the same final S_{55} value. By doing this for both fresh samples with various initial values of S_{44}, it was possible to adjust S_{44} until they both gave the same final S_{55} value; S_{55} and S_{44} then correctly corresponded to the given pair of M_z^0 values. The same was true for the x-axis samples using the M_x^0 pair and Equation 5. The results are given in Table I.

Then all of Wilson's measured M values [8] (Table II) were corrected to zero twist and infinite length. The mean ratio of M_z and M_x at zero twist to those at angle θ_{SM} varied linearly with θ_{SM} for each fresh sample (Fig. 6), but the gradient was greater for the wider samples. The simplest assumption was that this gradient was linearly related to the aspect ratio w/t; then Wilson's M values were corrected to zero twist (M^0, Table II). A similar procedure of linear interpolation and extrapolation from the S_{55} against l^{-1} gradients (Fig. 5) was needed to correct each of Wilson's M^0 values to

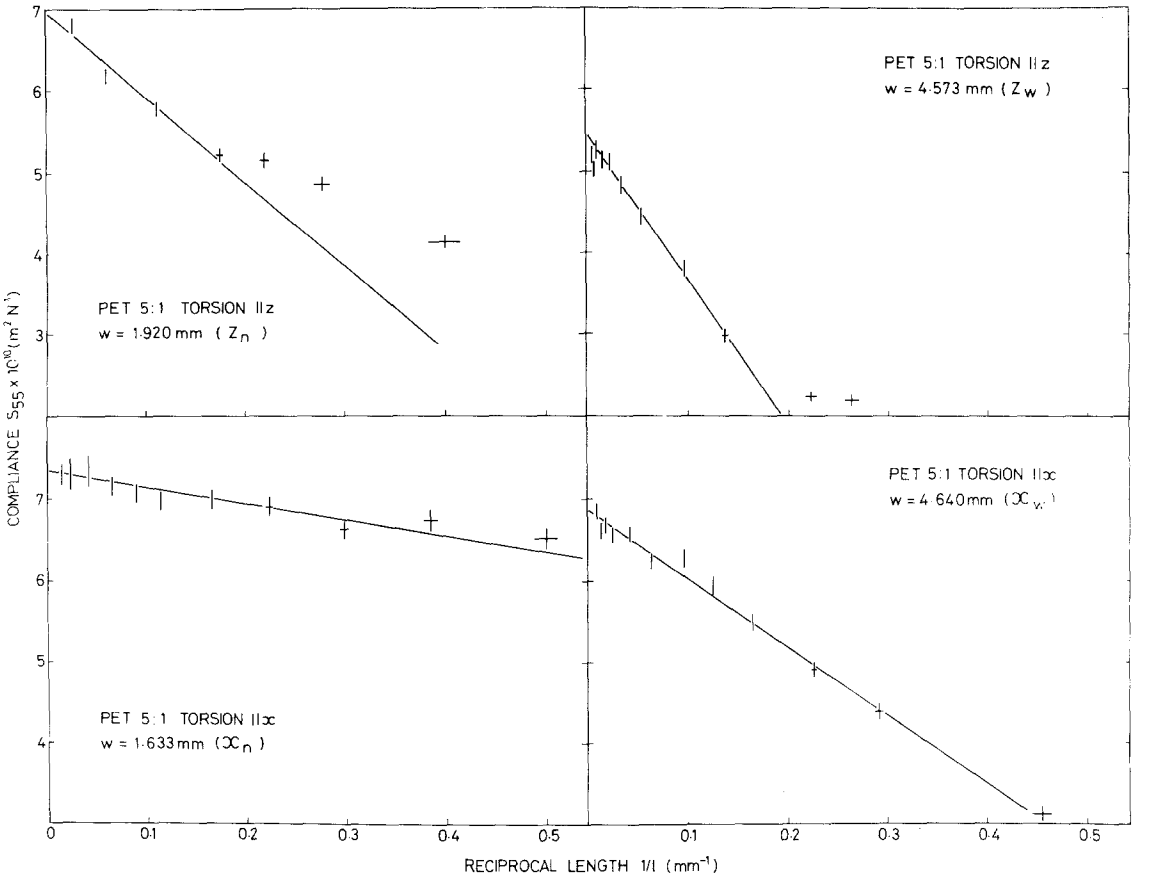

Figure 5 The overall elastic shear compliance S_{55} as a function of reciprocal length for the four fresh PET samples. Each point is accurate to within about 2% and the straight lines fitted to them by eye. Extrapolating back to zero reciprocal length gives end-free compliances.

infinite length. Then, using Wilson's initial values for S_{44}, S_{55} and S_{66}, the semi-exact [4, 14] and levelling methods [16] were used to refine these values to those corrected to zero twist and infinite length. The results are listed in Table II.

3.1.1. Errors in the torsion method

A full examination of the sources of error in the torsion method was made in previous work on nylon 6 by Lewis and Ward [16]. The reproducibility in the present work (internal consistency in the twist readings) was again about 0.4% at most lengths, rising to around 2% at the shortest lengths. Estimated errors in measuring the M values were 2.5% from all sources [8], plus an extra error of between 1.1 and 1.4% from the extrapolation to zero twist and infinite length. Errors in the sample dimensions were ± 1.5% in wt^3 and ± 0.05 mm in the length l. Errors in the treatment of the results added a further uncertainty of between 1.1 and

TABLE I Dimensions and results for the four fresh PET samples. R is the ratio of M value at Wilson's θ_{SM} to that at zero twist

Sample	w (mm)	w/t	M values from Wilson's compliances (N mm² rad⁻¹)	Factor R	Corresponding M^0 values (N mm² rad⁻¹)	M^0 at infinite length (N mm² rad⁻¹)	Resulting compliances ($\times 10^{-10}$ m² N⁻¹)
z_w z-axis wide	4.57	17.77	36.66	1.123 ± 0.005	41.16	39.50	$S_{55} = 5.57$
z_n z-axis narrow	1.92	7.23	12.97	1.059 ± 0.004	13.73	13.47	$S_{44} = 105$
x_w x-axis wide	4.64	18.21	35.20	1.075 ± 0.003	37.84	37.14	$S_{55} = 5.70$
x_n x-axis narrow	1.63	6.16	8.94	1.029 ± 0.003	9.20	9.05	$S_{66} = 143$

TABLE II Results for the set of samples examined by Wilson [8]; values M are his measured M values, and M^0 those calculated to zero twist (all in N mm^2 rad^{-1})

w (mm)	w/t	wt^3 (10^{-6} mm^4)	Wilson's M	M^0	M^0 at infinite length	Resulting compliances ($\times 10^{-10}$ m^2 N^{-1}) with standard errors
z-axis						
5.967	24.56	8.562	43.97	49.73	47.30	
4.994	20.72	6.990	35.41	39.58	37.89	$\overline{S_{44}^z} = 100 \pm 6$
3.800	15.77	5.319	24.60	26.96	26.10	
3.010	12.19	4.536	19.84	21.31	20.77	$\overline{S_{55}^z} = 5.47 \pm 0.19$
2.315	9.45	3.404	14.15	14.97	14.65	
1.942	7.89	2.891	11.41	12.02	11.80	
x-axis						
6.140	25.16	8.919	41.29	46.29	44.94	$\overline{S_{55}^x} = 5.81 \pm 0.22$
4.180	17.27	5.924	26.65	30.27	29.38	
3.111	12.86	4.409	17.24	19.09	18.63	$\overline{S_{66}^x} = 132 \pm 8$
2.022	8.39	2.830	9.97	10.86	10.72	

1.8% on the $\overline{S_{55}^z}$ and $\overline{S_{55}^x}$ values (from the spread in individual S_{55} calculated values), and 5% in the $\overline{S_{44}^z}$ and $\overline{S_{66}^x}$ values (from the maximum change in the ratios S_{55}/S_{44} or S_{55}/S_{66} before the plot of values calculated from Equations 4 or 5 could be seen to deviate from a horizontal straight line [16]). The total estimated standard errors are given in Table II. The difference between $\overline{S_{55}^z}$ and $\overline{S_{55}^x}$ is 0.34 ± 0.29 which is not statistically significant [24, 25] ($t = 1.2$, t-test) so that they were combined to give a final value for $\overline{S_{55}}$ of $(5.64 \pm 0.25) \times 10^{-10}$ m^2 N^{-1}.

3.1.2. Torsional end effects

The magnitude of effect 3 (see Section 2.3.1. of this paper) was next examined, to see how much it accounted for the total length effect seen. Effect 3 was chosen as it must be present in samples of rectangular cross-section. The Poisson's ratios for the material have already been measured [1, 2, 17]. For the 3 direction, $\nu_{13} = -S_{13}/S_{33} = 0.18/0.66 = 0.27$, and for the 1 direction, $\nu_{31} = -S_{13}/S_{11} = 0.18/3.61 = 0.050$. The correction factor Λ (Equation 2) was then calculated for the four fresh samples and applied to the measured compliances S_{55}^z or S_{55}^x at each length. The results are shown in Fig. 7. It can be seen that this correction accounts for all the effect in the x-axis samples down to an l/w ratio of about 4, and thereafter it over-corrects. However, there seem to be additional factors contributing to the z-axis results as the initial gradient of the line is still negative. This must be related to the low extension compliance S_{33} along this direction of 0.66×10^{-10} m^2 N^{-1}, compared with $S_{11} = 3.61 \times 10^{-10}$ m^2 N^{-1} (both corrected for end effects [17]), which would make effects 1 and 2 (see Section 2.3.1. of this paper) relatively more important. Here, for the z-axis, Λ starts to overcorrect at l/w ratios between 3 and 1. The values extrapolated to zero reciprocal lengths are, of course, unchanged.

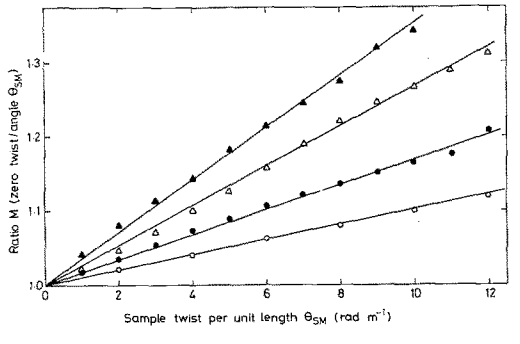

Figure 6 Behaviour of the ratio of M_z or M_x at zero twist to that at angle θ_{SM} with θ_{SM}: ▲ wider, z-axis (z_w); △ wider, x-axis (x_w); • narrower, z-axis (z_n); ○ narrower, x-axis (x_n).

3.2. Simple-shear results

For the simple-shear technique, fresh identical samples were cut from the same PET sheet I with the long axis parallel to the draw direction 3 (for S_{44}) or parallel to the transverse direction 1 (for S_{66}). Their mean dimensions were for S_{44}: $l = 20.28$, $w = 2.872$, $t = 0.256$ mm, and for S_{66}: $l = 20.28$, $w = 3.126$, $t = 0.253$ mm. They were mounted as in [5].

The lateral stress was adjusted to the maximum value to be used (about 5 MN m^{-2}) and the samples

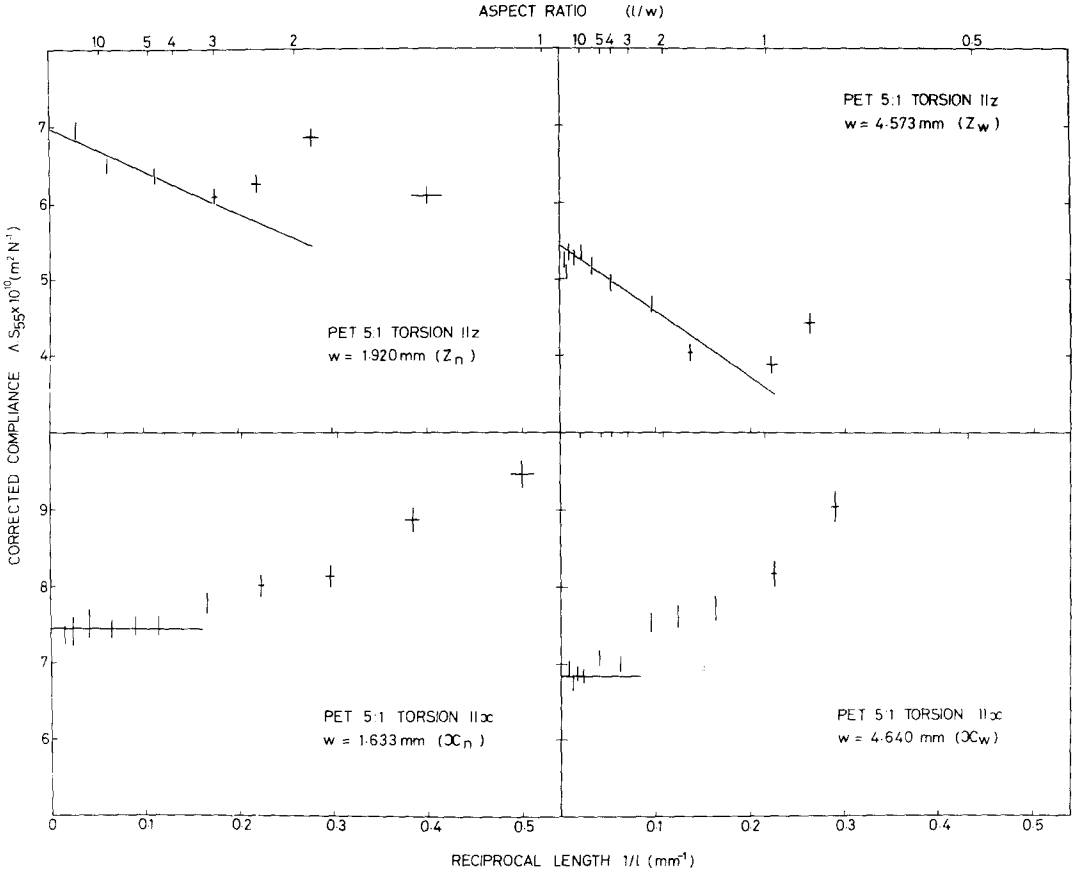

Figure 7 Overall elastic shear compliances S_{55} multiplied by Λ for the four fresh PET samples as a function of reciprocal length. The straight lines indicate that the correction is sufficient for the x-axis samples (lower pair of graphs) up to an aspect ratio l/w of about 4, but is not enough for the z-axis samples (upper pair).

then allowed to settle down for two or more hours. They were then conditioned mechanically to ensure reproducibility by applying about 80% of maximum load for 10 sec and then relaxing for 110 sec and repeating until the displacements were reproducible. Three such cycles were usually enough. The amount of creep was relatively small.

The shear displacements were then measured over a wide range of lateral stresses and up to 0.42% strain (S_{44}) or 0.50% strain (S_{66}). The samples were allowed to recover for two hours or more and reconditioned after each adjustment of lateral stress. Readings were taken 10 sec after applying the load and corrected for apparatus displacement [5]. The temperature was 20° C, and variations in sample compliance owing to small temperature changes (± 3° C) were negligible. The sample compliances were found to depend on strain (Fig. 8) and they were therefore extrapolated back to zero strain so that comparison with the torsional values was possible.

The results for S_{44} and S_{66} are presented in Fig. 9 which shows a behaviour of the sample compliance with σ_2 similar to isotropic PE [5]. The experimental points were fitted by least squares first to a straight line and then to a quadratic form. The values of the distribution χ_n^2

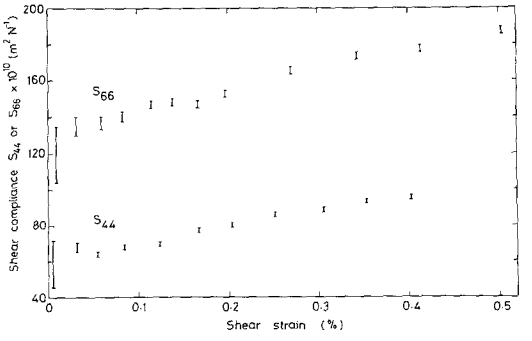

Figure 8 Typical variation of shear compliances S_{44} and S_{66} of PET with shear strain, from the simple-shear method.

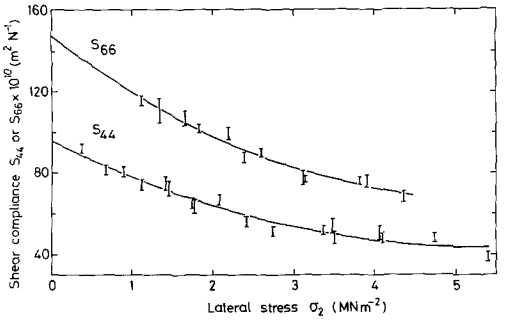

Figure 9 Shear compliances S_{44} and S_{66} of PET from the simple-shear method as a function of lateral stress. The curves are the result of quadratic least-squares fits to the experimental points.

were calculated from the deviations of the n points from the calculated line. The probability of a chance fit (p in Table III) was calculated from standard χ^2 tables [28]. The probability was found to be < 0.001 for each linear fit but showed that the quadratic fits gave adequate representations of the data [5]: these are the continuous lines in Fig. 9. Table III gives the results together with the values of S_{44} and S_{66} extrapolated to $\sigma_2 = 0$ from the quadratic procedure.

3.2.1. Errors in the simple-shear method

The sources of error are as follows: (a) extrapolation to zero stress, calculated from the deviation of the points from the fitted line; (b) errors in each point, from apparatus calibration, from measurement of the displacements and in removing the apparatus contribution, and from extrapolating the measured sample compliance to zero strain; (c) sample dimensions; (d) end effects; and (e) sample variability. End effects in simple-shear had been found to be negligible with samples 1.8 mm thick [5], and since the effect is likely to be even less with thinner samples, (the correction being of the form [25] $1 - \epsilon R(t/l)$, where $\epsilon R \leqslant 0.27$ and is smaller for smaller Poisson's ratios), it should be negligible here. Table III lists the magnitude of the sources of error, and the final error quotation, σ_t, is the total overall standard error obtained by combining the uncertainties (a), (b) and (c).

3.2.2. Creep and strain dependences

It was possible to measure the shear creep and stress–strain behaviour by the simple-shear technique, which is very difficult to do in torsion owing to the non-uniform stress distribution. The creep behaviour was obtained by noting the displacements as a function of time after loading, and the results for time dependence $\Delta_t S$ from 10 to 1000 sec [4, 5, 15, 16] are:

$$\Delta_t S_{44} \text{ at } 0.17\% \text{ strain} = (11 \pm 3)\%;$$

$$\Delta_t S_{66} \text{ at } 0.17\% \text{ strain} = (25 \pm 8)\%.$$

Strain dependences $\Delta_\epsilon S$ [16] were obtained from ten-second compliance against strain graphs such as Fig. 8, and the results are:

$$\Delta_\epsilon S_{44} = (27.0 \pm 3.0)\%; \quad (10 \text{ readings})$$

$$\Delta_\epsilon S_{66} = (32.7 \pm 1.7)\%, \quad (32 \text{ readings})$$

from zero to 0.4% strain.

4. Discussion

4.1. Comparison of shear compliance values

We may now compare the values for the shear compliances obtained by the two methods. The difference in the values of S_{44} from Tables II and III is $(4 \pm 7) \times 10^{-10}$ m^2 N^{-1}, and for S_{66} the difference is $(16 \pm 11) \times 10^{-10}$ m^2 N^{-1}. These differences are not statistically significant [26] (student's t-test [27]) and so we can consider that all the results lie in the same population. This increases our confidence in the validity of both techniques for determining the shear compliances of the uniplanar-axially-oriented material. Thus, we may take the weighted mean for the two methods to give the final values for the shear compliances of this PET sheet; these appear in Table IV.

The end effects in torsion about the x-axis are adequately accounted for solely by the warping

TABLE III Results for the curve-fitting, uncertainties, and compliances for simple-shear experiments on PET samples. The sources of error are as follows: (a) quadratic extrapolation to $\sigma_2 = 0$; (b) R.M.S. error of the measurement points; (c) sample dimensions; σ_t is the final overall standard error

Sample for compliance	Number of points (n)	Linear fit $\chi^2_n\, p(n-2)$	Quadratic fit $\chi^2_n\, p(n-3)$	Standard errors (a)	(b)	(c)	Compliances, at $\sigma_2 = 0$, $\pm \sigma_t$ ($\times 10^{-10}$ m^2 N^{-1})
S_{44}	18	$72 < 0.001$	$34 \sim 0.01$	± 2.8	± 2.7	0.56%	95.9 ± 3.9
S_{66}	12	$48 < 0.001$	$19 \sim 0.04$	± 6.5	± 3.1	0.55%	147.6 ± 7.2

TABLE IV The full set of compliances for the drawn PET sheet I, all corrected for end effects. The error estimates are one standard error

Compliance	Value ($\times 10^{-10}$ m^2 N^{-1})
S_{11}	3.61 ± 0.12
S_{22}	9.0 ± 1.6
S_{33}	0.66 ± 0.01
S_{12}	−3.8 ± 0.4
S_{13}	−0.18 ± 0.01
S_{23}	−0.37 ± 0.05
S_{44}	97 ± 3
S_{55}	5.64 ± 0.25
S_{66}	141 ± 8

effect 3 (see Section 2.3.1. of this paper). Thus, for materials with an extensional compliance similar to S_{11} here, and of similar dimensions, applying Equation 2 should be sufficient to correct for torsional end effects. The z-axis results, however, have contributions from the other two effects as well, owing to the low value of S_{33}. However, an empirical extrapolation to zero reciprocal length will always give end-free results.

4.2. The overall mechanical anisotropy and its relationship to structure

The determination of the three shear compliances completes the determination of the nine independent compliances for this sheet (Table IV). It shows a very high degree of mechanical anisotropy, and the two major structural features, the high chain-axis orientation and the preferential orientation of the (0 0 1) planes (which mainly reflect preferential orientation of the terephthalate residues in the PET chain), are directly reflected in the anisotropy. Infra-red measurements [29] have shown that the high degree of chain orientation is linked with a very high proportion of glycol residues in the extended-chain trans-conformation. The low value of the extensional compliance S_{33} can then be explained by supposing that the deformation involves some bond stretching and bending in the extended-chain molecules of PET in the highly-oriented structure. These molecules could be the taut tie-molecules of Peterlin [30]. On the other hand, the transverse compliances S_{11} and S_{22} are approximately an order of magnitude greater, which is consistent with the lower stresses relating to dispersion forces.

The anisotropy of the shear compliances is perhaps the most marked feature of the results. Both S_{44} and S_{66} appear to reflect easy shear in the 23 and 12 planes respectively, presumably where the planar terephthalate chains are sliding over each other constrained only by weak dispersion forces. The compliance S_{55}, on the other hand, which geometrically involves distortion of the molecular plane, is of a similar order of magnitude to S_{11} and S_{22}.

Earlier work has shown that the mechanical anisotropy of PET is affected by molecular orientation rather than by crystallinity [31, 32]. This led to the proposition of the aggregate model [31–34], in which the polymer is regarded as an aggregate of anisotropic units which are aligned by drawing. The compliances of the isotropic polymer were then predicted to lie between two bounds, Reuss (assuming uniform stress) and Voigt (uniform strain), obtained by averaging the compliance constants or the stiffness constants of the anisotropic unit. In these earlier works [31–35] the elastic constants of the unit were assumed to be those of the most highly oriented fibre which could be obtained, and it was shown that the measured elastic constants for an isotropic fibre lay between the predicted bounds. A similar result is obtained if the present data for the one-way-drawn sheet are used to calculate the Reuss and Voigt bounds (Table V). A further test of the aggregate model is to calculate bounds for the elastic constants of an "equivalent fibre", by averaging the film constants in the plane normal to the film draw direction. The results of this calculation are shown in Table VI together with the experimental values obtained for a highly-oriented monofilament [9, 35]. Although the experimental values do not always lie exactly within the predicted bounds, they are always in the correct range. Taking into account the very large degree of anisotropy and the very simplistic nature of these calculations, it is considered that these results afford good support for the contention that to a first approximation the mechanical anisotropy can be considered in terms of the single-phase aggregate model.

TABLE V Comparison of calculated and measured compliance constants ($\times 10^{-10}$ m^2 N^{-1}) for isotropic PET polymer based on sheet compliances

Compliance constant	Calculated bounds		Experimental value
	Reuss	Voigt	
S_{33}	15	2.7	4.4
S_{44}	51	7.2	11

TABLE VI Comparison of calculated and measured compliance constants ($\times 10^{-10}$ m^2 N^{-1}) for highly-oriented PET fibres based on sheet compliances

Compliance constant	Calculated bounds		Experimental value
	Reuss	Voigt	
S_{11}	20	8.1	16.1
S_{12}	−18	−6.0	−5.8
S_{13}	− 0.28	−0.25	−0.31
S_{33}	0.76	0.76	0.71
S_{44}	51	11.5	13.6

5. Conclusions

(1) End effects in the torsion of flat anisotropic PET sheets are small and can be readily dealt with by the analysis based on the block model of Folkes and Arridge [23]. Our results suggest that the end effects penetrate further into the sample in the draw direction than in the transverse direction, and this supports Horgan's theoretical analysis of their propagation in anisotropic materials [19, 20].

(2) The recently-developed simple-shear method has been used to determine the shear compliances S_{44} and S_{66} for uniplanar-axially-oriented PET sheet.

(3) The results for the shear compliances S_{44} and S_{66} obtained by torsion and simple shear agree well, increasing confidence in both methods.

(4) The determination of the shear compliances completes the determination of all nine independent elastic constants for the PET sheet. The values have been used to predict bounds for isotropic PET and an "equivalent fibre", based on the single-phase aggregate model. The results confirm that this model gives a reasonable first approximation to an understanding of the mechanical anisotropy of PET. In structural terms this has been taken to imply that molecular orientation rather than morphology *per se* is important in determining the mechanical behaviour of this polymer.

Acknowledgement

ELVL would like to thank the Science Research Council for financial support during the course of this work.

References

1. I. WILSON, N. H. LADIZESKY and I. M. WARD, *J. Mater. Sci.* **11** (1976) 2177.
2. I. WILSON, A. CUNNINGHAM and I. M. WARD, *ibid.* 2181.
3. I. WILSON, A. CUNNINGHAM, R. A. DUCKETT and I. M. WARD, *ibid.* 2189.
4. N. H. LADIZESKY and I. M. WARD, *ibid.* 8 (1973) 980.
5. E. L. V. LEWIS, I. D. RICHARDSON and I. M. WARD, *J. Phys. E.* **12** (1979) 189.
6. N. BROWN, R. A. DUCKETT and I. M. WARD, *Phil. Mag.* **18** (1968) 483.
7. M. KASHIWAGI, A. CUNNINGHAM, A. J. MANUEL and I. M. WARD, *Polymer* **14** (1973) 111.
8. I. WILSON, "The Mechanical Anisotropy of Oriented Polyethylene Terephthalate Sheet", Ph.D. Thesis, University of Leeds (1977).
9. I. M. WARD, *Plastics and Rubber: Materials and Applications* **2** (1977) 141.
10. C. J. HEFFELFINGER and R. L. BURTON, *J. Polym. Sci.* **47** (1960) 289.
11. M. CASEY, *Polymer* **18** (1977) 1219.
12. H. J. BIANGARDI and H. G. ZACHMANN, *J. Polym. Sci. Polym. Symposium* **58** (1977) 169.
13. G. RAUMANN, *Proc. Phys. Soc.* 79 (1962) 1221.
14. N. H. LADIZESKY and I. M. WARD, *J. Macromol. Sci.-Phys.* **B5** (1971) 745.
15. *Idem, ibid.* **B9** (1974) 565.
16. E. L. V. LEWIS and I. M. WARD, *ibid.*, in press.
17. E. L. V. LEWIS, *J. Mater. Sci.* **14** (1979) 2343.
18. S. P. TIMOSHENKO and J. N. GOODIER, "Theory of Elasticity", Third Ed. (McGraw-Hill, New York, 1970) Chap. 10.
19. C. O. HORGAN, *J. Elasticity* **2** (1972) 169, 335.
20. *Idem, Int. J. Solids Struct.* **10** (1974) 837.
21. I. CHOI and C. O. HORGAN, *J. Appl. Mech.* **44** (1977) 424.
22. *Idem, Int. J. Solids. Struct.* **14** (1978) 187.
23. M. J. FOLKES and R. G. C. ARRIDGE, *J. Phys. D.* 8 (1975) 1053.
24. J. J. BIKERMAN, "The Science of Adhesive Joints" Academic Press, New York and London, 1961) Chap. 7.
25. W. T. READ, *J. Appl. Mech.* **17** (1950) 349.
26. J. TOPPING, "Errors of Observation and their Treatment", Third Ed. (The Institute of Physics and The Physical Society, London, 1962).
27. M. J. MORONEY, "Facts from Figures", Second Ed. (Penguin Books, London, 1953) Chap. 13.
28. R. A. FISHER and F. YATES, "Statistical Tables", Fourth Ed. (Oliver & Boyd, Edinburgh, 1953).
29. A. CUNNINGHAM, I. M. WARD, H. A. WILLIS and V. J. I. ZICHY, *Polymer* **15** (1974) 749.
30. A. PETERLIN, "Ultra High Modulus Polymers", edited by A. Ciferri and I. M. Ward (Applied Science Publishers, London, 1979) p. 292.
31. I. M. WARD, *Text. Res. J.* **31** (1961) 650.
32. P. R. PINNOCK and I. M. WARD, *Proc. Phys. Soc.* **81** (1963) 260.
33. I. M. WARD, *ibid.* **80** (1962) 1176.
32. I. M. WARD, "Mechanical Properties of Solid
34. *Idem*, "Mechanical Properties of Solid Polymers" (John Wiley and Sons, New York, 1971) p. 253.
35. I. M. WARD, *Polymer* **15** (1974) 379.

Received 24 September 1979 and accepted 18 February 1980.